Ablation and optical property modification of transparent materials with femtosecond lasers

M. Richardson*, A. Zoubir, L. Shah,
Laser Plasma Laboratory
and
C. Rivero, C. Lopez, K. Richardson
Glass Processing & Characterization Laboratory

School of Optics & CREOL, University of Central Florida,
Orlando, Florida 32816. USA

and

N. Hô, R. Vallée
Département de Physique and Centre d'Optique Photonique et Laser
Université Laval, Quebec, Canada

Abstract

Because of the unique laser–matter interaction processes involved, femtosecond laser micro-machining and femtosecond laser materials processing techniques are developing rapidly to stages where they may be introduced into manufacturing. Yet in both these areas, some complex interaction phenomena are not fully understood. In this talk we describe two studies of fundamental processes that impact both of these areas. These studies were made in transparent media, but their findings will be applicable to many non-transparent materials.

Micro-machining in confined regions can give rise to new physical mechanisms emerging to dominate the machining process. We show this occurs in deep hole drilling of glasses by femtosecond laser pulse, where self-focusing effects takes over in the ablating process. The conditions under which this occurs will be described, and other configurations discussed where these phenomena may be important.

At intensities below that required for ablation, structural modification of materials may be effected by femtosecond laser pulses. This has opened pathways towards direct femtosecond laser writing of optical waveguides, micro-fluidic systems and other structures. We will describe the controlled variation of refractive index that can be created in certain types of glasses and there potential for optical waveguides, and active optical elements. The evolution of these techniques will lead to their eventual integration for the fabrication of multi-component systems on a single chip.

Laser-Induced Damage in Optical Materials: 2003, edited by G. J. Exarhos, A. H. Guenther, N. Kaiser, K. L. Lewis, M. J. Soileau, C. J. Stolz, Proceedings of SPIE Vol. 5273 (SPIE, Bellingham, WA, 2004) · 0277-786X/04/$15 · doi: 10.1117/12.530684

1.0 INTRODUCTION

Femtosecond laser micromachining shows promise for many fields including in micro-optics, micro-electronics, micro-biology and micro-chemistry. Because of its non-contact nature, laser ablation allows micromachining and surface patterning of materials with minimal mechanical and thermal deformation. For some applications the femtosecond regime offers advantages over the nanosecond regime. These stem from the short energy time, too short for thermal diffusion to occur. As a result, the heat-affected zone (HAZ), where melting and re-solidification occur, is significantly reduced, leading to smaller structured features having higher aspect ratios, and greater spatial precision. A second advantage of femtosecond laser micromachining is its versatility in range of materials that can be processed. Femtosecond laser micro-machining is applicable to metals, semiconductors, polymers, oxide ceramics, silica aerogels, optical glasses and crystals, and lends itself to a variety of processing that include the fabrication of photonic crystals[1], data storage, fabrication of waveguides[2], gratings and single mode couplers[3]. Here we describe femtosecond laser micromachining of different materials from three perspectives, (i) deep hole penetration in optical glasses and composite materials, (ii) the fabrication of microscopic gratings by high repetition-rate ablation and (iii) the creation of waveguides, in chalcogenide glass As_2S_3 thin films. Deep hole drilling is characterized by measuring the maximum laser penetration depth in a variety of glasses. The waveguide and grating fabrication by femtosecond laser writing is characterized using a standard interferometric microscope. Insight on the photorefractive mechanism caused by a femtosecond pulse is given by Raman spectra of guided light.

There are several mechanisms that govern femtosecond laser ablation. Upon irradiation, bound and free electrons in the surface layer of the material; are excited via multi-photon absorption[4]. Hot electrons are generated, the material becomes ionized and a plasma forms on the surface. The energy is then transferred to the lattice through bond breaking and material expansion. Because these processes occur on a picosecond time scale, thermal diffusion into the material is nearly negligible. Thermal relaxation is characterized by the thermal diffusion length D related to the pulse width τ_p by $D = \kappa\tau_p^{1/2}$, where κ is the thermal diffusivity of the material[5]. If D is shorter than the absorption length, ablation precedes thermal diffusion and the material does not have time to melt and re-solidify. In the nanosecond regime, it is generally accepted that ablation begins with the ionization of surface carriers, which are typically defects or impurities[6]. Due to the non-uniform distribution of surface carriers in dielectrics, experiments have demonstrated that no precisely-defined laser-induced damage threshold exists for laser pulses longer than 10 ps. By contrast, ultrashort laser pulses (<200 fs), with target intensities often in excess of 10^{12} W/cm^2, are capable of freeing bound electrons via Multi-Photon Ionization (MPI). Experiments have shown that the laser-induced damage threshold for an ultrashort laser pulse has a precise value corresponding to the onset MPI, completely determined by the ionization bandgap energy of the target material.

2.0 DEEP HOLE DRILLING IN SILICATE GLASS

Here we demonstrate that femtosecond laser pulses from a regeneratively amplified Ti:Sapphire laser can be used to drill holes (≥1 mm in depth) with high aspect ratio (≥10:1) in transparent materials at atmospheric pressure with high ablation rates, that is, high processing speeds.

We have investigated the laser ablation of two silicate glasses in three different laser ablation scenarios: with a femtosecond laser at 845 nm, with a nanosecond laser at 845 nm and with a nanosecond laser at 1064nm. In order to study the influence of the ionization bandgap on laser ablation, soda-lime glass (~5 eV) and 45%mol. PbO lead-silicate glass (~2.5 eV) were examined[7]. Ablation is performed at atmospheric pressure in two regimes, that is, below and above the air ionization threshold intensity, to gauge how air-ionization modifies the hole profile and material removal rate. The femtosecond laser system was a Kerr-lens modelocked Ti:Sapphire oscillator regeneratively amplified by a flashlamp pumped Cr:LiSAF amplifier, able

to produce 110 fs (FWHM) laser pulses with a Gaussian temporal profile at 845 nm. The second laser was the unseeded CrLiSAF regenerative amplifier, which produces long (60 ns) Q-switched pulses, at 845 nm, from which square 10 ns pulses are sliced using an extra-cavity Pockels cell as an electro-optical pulse cutter. The third laser was a flashlamp-pumped Q-switched Nd:YAG laser that produced 15 ns (FWHM) Gaussian-shaped laser pulses at 1064 nm. The laser parameters are listed in Table 1. For each test, the laser beam was expanded using a 4:1 telescope and filtered by an iris. It is then focused to a 100μm diameter spot onto the target using a fused silica plano-convex lens with a 20 cm focal length. After initial positioning, the focus spot was not moved during the ablation. The holes are drilled parallel to the long axis of thin polished glass plates.

Table 1 – Laser parameters

Laser	Wavelength λ (nm)	Pulse Duration t_p Pulse Energy, E_p	Repetition Rate, R (Hz)	Focal Spot Diameter, D (μm)	Laser Fluence, F_p (J/cm^2)	Focal Intensity, I_p (W/cm^2)
Ti:Saph/ Cr:LiSAF	845	110 fs (FWHM) 1.5 mJ	5	100 (FW1/e^{2}M)	19.1	1.74x10^{14}
Cr:LiSAF	845	10 ns (FWHM) 4.0 mJ	5	100 (FW1/e^{2}M)	51.0	5.10x10^9
Nd:YAG	1064	15 ns (FWHM) 2.2 mJ	10	100 (FW1/e^{2}M)	28.0	1.87x10^9

Optical microscope images of the holes produced by 10^4 laser pulses in soda-lime silicate glass and PbO lead-silicate glass are shown in Figs. 1 and 2.

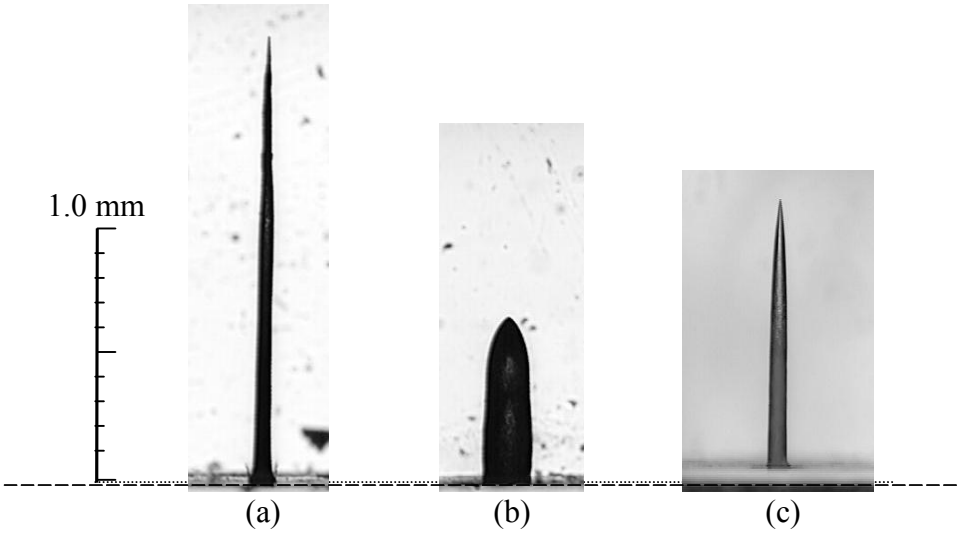

Fig. 1: Hole profiles in soda-lime glass produced by 10^4 laser pulses
a) λ = 845 nm, t_p = 110 fs, E_p = 1.5 mJ, I_p = 1.74x10^{14} W/cm^2, F_p = 19.1 J/cm^2
b) λ = 845 nm, t_p = 10 ns, E_p = 4.0 mJ, I_p = 5.10x10^9 W/cm^2, F_p =51.0 J/cm^2
c) λ = 1064 nm, t_p = 15 ns, E_p = 2.2 mJ, I_p = 1.87x10^9 W/cm^2, F_p =28.0 J/cm^2

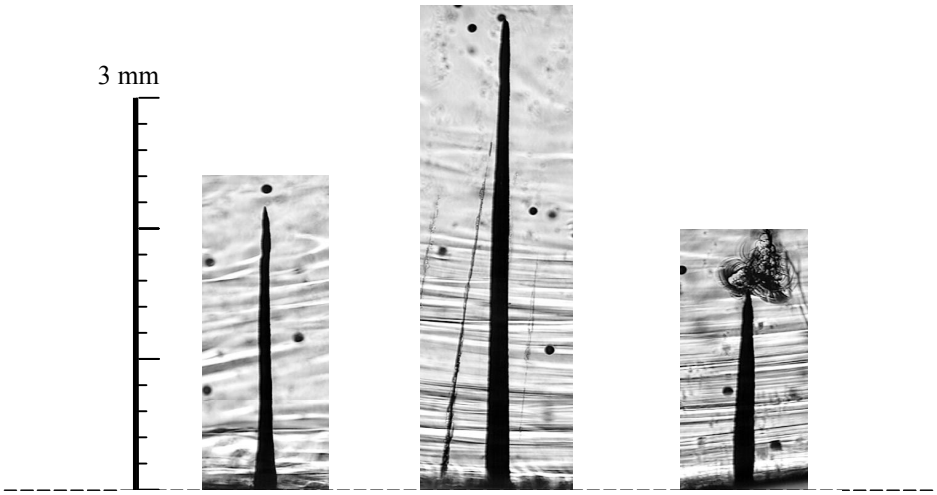

Fig. 2: Hole profiles in 45% mol. lead silicate glass produced by 10^4 laser pulses
a) λ = 845 nm, t_p = 110 fs, E_p = 1.5 mJ, $I_p = 1.74 \times 10^{14}$ W/cm^2, F_p = 19.1 J/cm^2
b) λ = 845 nm, t_p = 10 ns, E_p = 4.0 mJ, $I_p = 5.10 \times 10^9$ W/cm^2, F_p =51.0 J/cm^2
c) λ = 1064 nm, t_p = 15 ns, E_p = 2.2 mJ, $I_p = 1.87 \times 10^9$ W/cm^2, F_p =28.0 J/cm^2

The overall penetration depth was significantly greater for PbO lead-silicate than for soda-lime silicate glass in the three different ablation scenarios due to a higher Z resulting in a higher electron density. In addition, there is a drastic difference in hole depth and width between Figure 2b and Figure 2c, which illustrates the variations in ablation mechanism and hole morphology obtained in the nanosecond regime at 845 nm and 1064 nm. Furthermore, in both materials, the femtosecond ablation is more energetically efficient as greater penetration depths are obtained with a smaller energy per pulse.

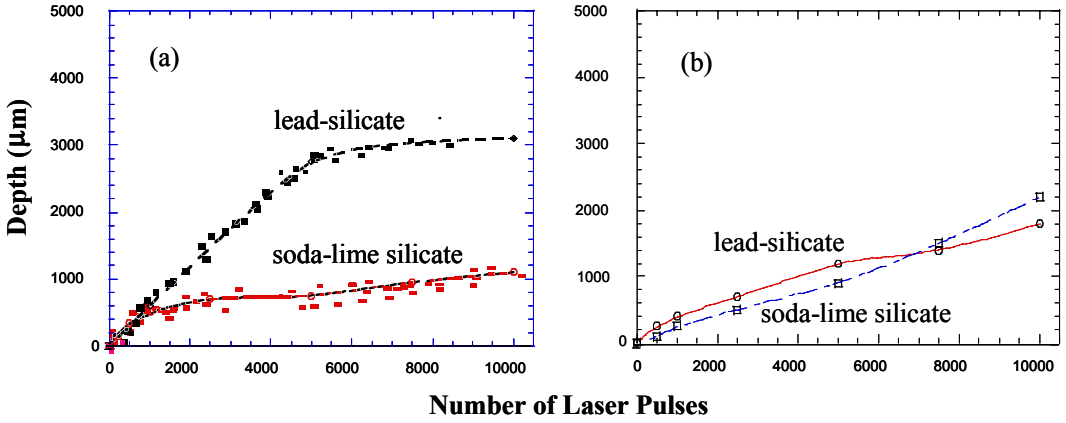

Fig. 3 Laser penetration depth vs. number of incident laser pulses (t_p = 110 fs, λ = 845 nm, E_p = 1.5 mJ) given: (a) $I_p = 3.08 \times 10^{14}$ W/cm^2, F_p = 33.9 J/cm^2, and d = 75 µm (FW1/e^{2}M): (b) $I_p = 1.74 \times 10^{14}$ W/cm^2, F_p = 19.1 J/cm^2, and d = 100 µm (FW1/e^{2}M)

Similar tests were made in the femtosecond regime with fluences sufficient to ionize the air. The fluence of the laser was increased by reducing the beam spot size from 100 μm to 75 μm. a comparison of the ablation of the two silicate glasses below and above the air ionization threshold is shown in Fig.3 Below the air ionization threshold, the ablation rate remained constant over the tested range at ~0.2 μm/pulse for both glasses. Above the air breakdown threshold, the ablation rate rises up to ~0.5 μm/pulse and rapidly reduces down to ~0.05 μm/pulse, but for ~1000 shots for soda-lime and for ~5000 shots for PbO silicate glass. There is a striking increase in the ablation-rate for the PbO glass at higher intensities. There are number of possible explanations for this. Firstly, we know that the influence of the air ionization makes a change to the ablation rate[8]. However, the interaction physics with the higher Z glass could also be playing a role, and one cannot exclude the possible differences in material properties.

Optical probe images, taken during the laser material interaction above ionization threshold, revealed that after a certain depth is achieved, light starts to form a thin (~10 μm) hot filament confined inside the hole (Fig.4) High-intensity ultrashort laser pulses propagating in air have been observed to self-channel into light filaments exceeding the Raleigh length[9]. It is believed that a similar effect occurs because of evaporated material that remains temporarily confined in the hole, thus increasing the nonlinear index of refraction of the atmosphere. More evidence of this effect is present in Fig. 5 where very sharp holes pointing in slightly different directions are shown at the tip of the hole both in lead silicate glass and As_2S_3, a chalcogenide glass. These pins could be attributed to ablation due to self-channeled single shots. Note that the individual pins or filaments in the material are uniformly ~ 100 μm long. In addition, it is important to note that the rollover in the ablation rate described above occurred earlier for PbO lead silicate than for soda-lime silicate. The presence of high Z elements (PbO) or particles of highly non linear material (As_2S_3) in the hole atmosphere can account for a higher nonlinear index of refraction, thus lowering the intensity threshold for self-focusing.

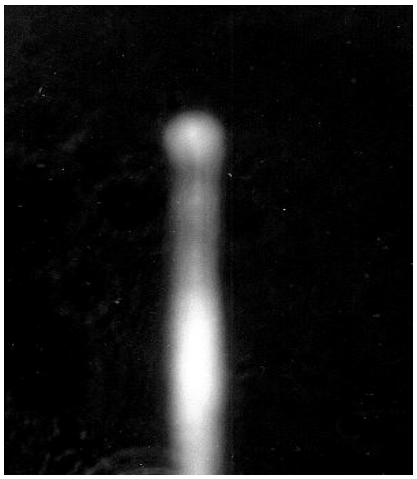

Fig. 4– Hot filament inside an ablated hole in lead silicate glass

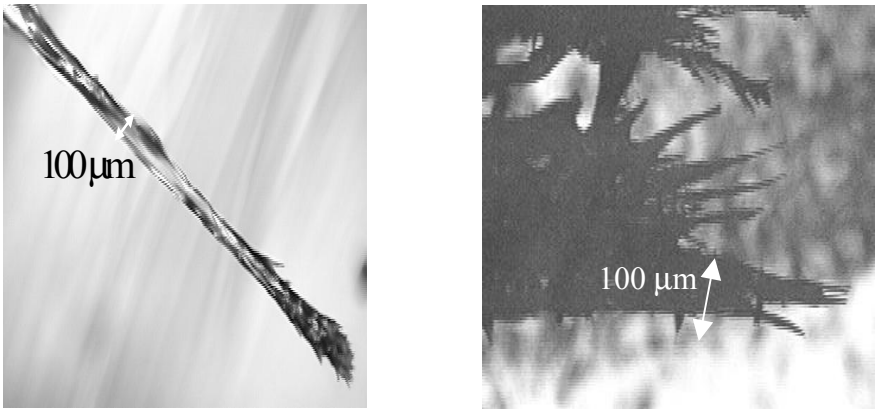

Figure 5 – Evidence of self-focusing in lead silicate and chalcogenide glass

3.0 HOLE DRILLING IN COMPOSITE MATERIAL

As an illustration of how effective femtosecond lasers are for micro-machining complex structures, Fig. 6 shows holes drilled in 3 mm thick graphite fiber composite material with nanosecond and femtosecond lasers. While the nanosecond regime yields dislocation of horizontal and vertical striations indicative of extent of heat-affected zone, the femtosecond regimes shows a clean, reproducible hole structure, without evidence of collateral surface damage. The difference in the size of the heat-affected zone is expected to be even greater in laminate materials where the heat caused by long pulses can only diffuse in two dimensions versus three in bulk material.

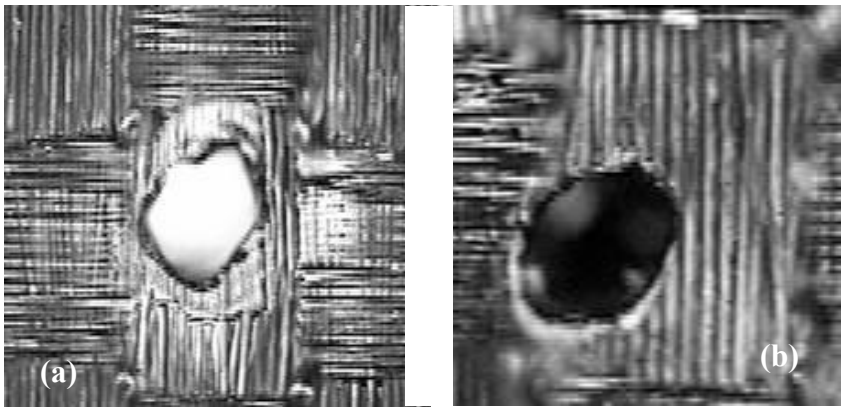

Fig.6 – 100x70 μm ablated hole in graphite fiber composite material
(a) Conventional nanosecond laser 1300 pulses with ~ 3.5 mJ/pulse
(b) 100 fs laser pulses in air, ~ 1 mJ/pulse

4.0 GRATING FABRICATION IN As_2S_3 CHALCOGENIDE GLASS THIN FILMS

We have also explored another regime of micro-machining with femtosecond laser pulses. In this regime the material is irradiated with a tightly-focused laser beam of femtosecond laser pulse with energies in the nanojoule range. In this regime each point on the surface of the material is irradiated with many laser pulses (10^4 – 10^6), at intervals of less than 1 μs between pulses. This mode of machining has the advantage of using much less complex laser technology: un-amplified femtosecond lasers can produce optical breakdown and structural change in bulk transparent materials using tightly focused pulses of just 5 nJ[10]. Using an

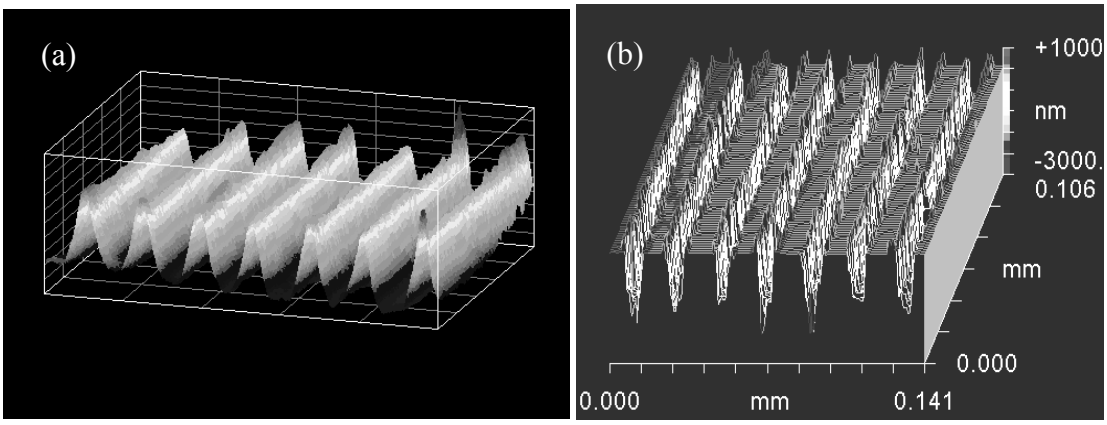

Fig.7 – Surface profile of (a) the phase and (b) relief grating on the As_2S_3 film produced with sub-50 fs laser pulses from the extended cavity un-amplified Ti:Sapphire oscillator

extended cavity un-amplified Kerr-lens mode-locked Ti:Sapph laser, relief and volume gratings with a 20 μm period were fabricated on a 1.66 μm thick, As_2S_3 thin film. The laser emission has a spectral

bandwidth of approximately 40 nm (FWHM) centered at 800 nm and a repetition rate of 28 MHz and produces pulses of sub-50 fs pulse duration. The system has an average output power of 0.55 W and produces energies up to 20 nJ/pulse. The output of the laser was focused by a 15X, 0.28NA reflective objective onto a target attached to a 3D motorized translation system. The sample was processed in two regimes (Fig. 7): Firstly, the intensity was kept below the ablation threshold, generating a volume grating resulting from photo-expansion and an induced index change, as observed through an interferometric microscope. In the second regime, intensities *above* the ablation threshold produced a relief grating with grooves of 0.2 μm depth

5.0 WAVEGUIDE FABRICATION IN BULK AND THIN FILM CHALCOGENIDE GLASSES

As illustrated above, a regime exists where the optical properties of the material can be altered, without drastically damaging the mechanical structure of the glass matrix. The obtained structures, as shown in Fig. 7a, exhibit rather smooth features with no heat affected zone and associated cracks surrounding the processed area. In addition, the exposed region exhibits an increase in refractive index. This regime is particularly advantageous for the fabrication of waveguides. Fig.8. shows a single channel waveguide fabricated in bulk 90%(GeS_2)-10%(Sb_2S_3) material. In this case, the sample was translated along the direction of the beam. In this configuration, also called longitudinal writing, the cross-section of the guide is circular and the waveguide length is limited by the microscope objective working distance, in this case 5 mm.

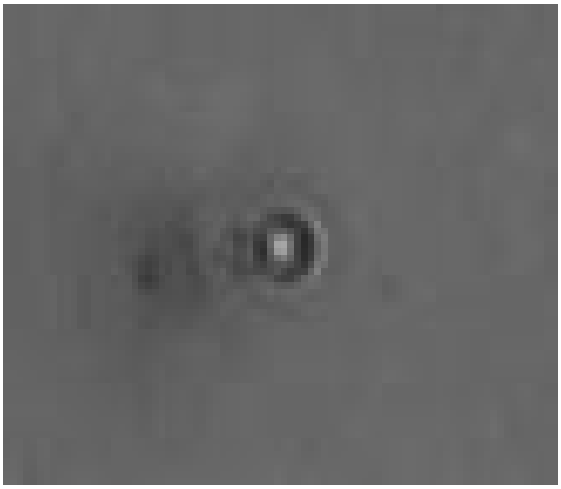

Fig. 8. Cross section of a longitudinal waveguide written in bulk 90%(GeS_2)-10%(Sb_2S_3)

In transverse writing, the sample is translated in a direction perpendicular to the laser beam. The translation speed is varied between 0.1 and 20 mm/s allowing the number of pulses incident on the laser focal spot area to be varied for different laser intensities. The laser intensity is adjusted with a variable metallic neutral density filter, placed before the microscope objective. The experiment is performed with a pulse rate of 10^4 - 10^6 pulses per focal spot and intensities in the range of 0-0.3 GW/cm^2.

The refractive index change Δn induced inside the waveguide is measured with the same technique used for the volume gratings. Measurements are made of its dependence on the laser irradiating intensity and the integrated absorbed laser flux density. The latter is shown in Fig 9(a) for As_2S_3 film. The value of Δn increases approximately logarithmically when the integrated laser flux density is increased by decreasing the translation speed. The Δn value shows a much sharper dependence on the pulse intensity for a constant translation speed as shown in Fig. 9(b). Clearly evident is the presence of an onset threshold for index modification, in this case at ~0.15 GW/cm^2 for As_2S_3. Since the exposure photon energy is well below the absorption edge of the material, this result strongly suggests that the mechanisms responsible for the structural and photo-induced refractive index changes rely on non-linear optical processes.

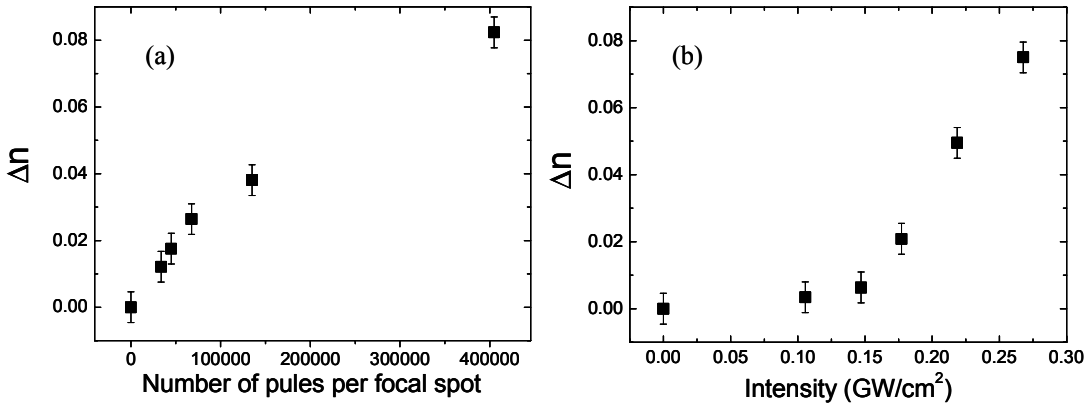

Fig. 9. Measured Δn versus (a) the number of pulses (pulse intensity is set to 0.25 GW/cm^2) and (b) the pulse intensity in As_2S_3 films

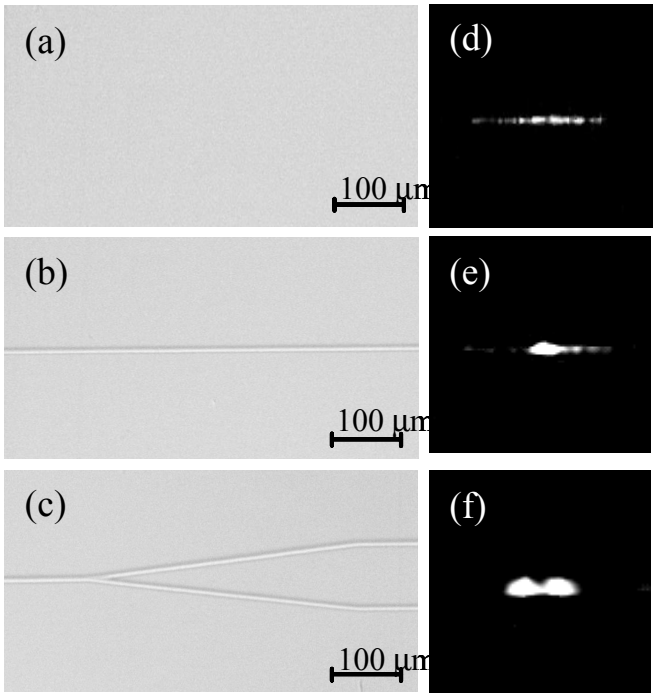

Fig. 10. Differential interference contrast microscope images of (a) the unexposed As2S3 films (b) a single-channel waveguide and (c) a Y-coupler. The insets (d), (e), (f) are CCD images of the near-field pattern of the coupled modes

Waveguides as long as 2 cm have been fabricated, this length only being limited by the range of the translation stage and the sample size. The waveguides are visualized with a differential interference contrast microscope having a magnification of 20X that identified the photo-induced change (Fig.10(a-c)). Characterization of the guiding properties of the waveguides produced is made by butt-coupling a 785 nm single-mode pigtailed laser diode to the cleaved waveguides. The near-field pattern of the coupled modes is then imaged onto a CCD (Fig. 10(d-f)). Coupling into As_2S_3 thin films is limited by the high refractive index of the material (n=2.45) which produces high Fresnel losses at both ends of the waveguide and mode-matching a single mode fiber to a rectangular waveguide. However, more than 70% of the light exiting the film end face (channel and film) was confined in the channel waveguide. Only a small fraction of the light

either did not couple due to mode mismatch, or was decoupled due to scattering. The measured ratio of power coupled in the two output branches of the Y-coupler was near 50%-50%.

6.0 CONCLUSION

This study has shown the ability of femtosecond material micro-processing to produce very fine surface structures. These structures can be created by ablation or by structural material modification. Femtosecond lasers have distinct advantages over nanosecond lasers for some types of micro-machining, because of the reduced heat deposition and the reduction of the HAZ. We have also demonstrated micro-machining in two laser processing regimes, one in which individual laser pulses interact with the material at low pulse repetition rates (1 – 1 kHz), and a second in which the material is processed by many laser pulses at high (> 1MHz) repetition rates. Finally in the latter regime, it is possible to uniquely change the material structure of some materials, at intensities below that required for ablation. We have demonstrated the fabrication of efficient optical waveguides in this regime.

7.0 REFERENCES

1. Sun, H.-B. ; Xu, Y.; Juodkazis, S.; Sun, K.; Watanabe, M.; Matsuo, S.; Misawa, H.; Nishii, J., "Arbitrary-lattice photonic crystals created by multiphoton microfabrication", *Optics Letters*, **Vol. 26**, Issue 6, pp. 325-327, 2001.
2. Hirao, K.; Miura, K., "Writing waveguides and gratings in silica and related materials by a femtosecond laser", *Journal of Non-Crystalline Solids*, **Vol. 239**, Issue 1-3, pp. 91-95, 1998.
3. Minoshima, K. ; Kowalevicz, A.M.; Hartl, I.; Ippen, E.P.; Fujimoto, J.G., "Photonic device fabrication in glass by use of nonlinear materials processing with a femtosecond laser oscillator", *Optics Letters*, **Vol. 26**, Issue 19, pp. 1516-1518, 2001.
4. Korte, F. ; Adams, S.; Egbert, A.; Fallnich, C.; Ostendorf, A.; Nolte, S.; Will, M.; Ruske, J.-P.; Chichkov, B.N.; Tunnermann et al., "Sub-diffraction limited structuring of solid targets with femtosecond laser pulses", *Optics Express*, **Vol. 7**, Issue 2, 2000.
5. Matthias, E. ; Reichling, M.; Siegel, J.; Kading, O.W.; Petzoldt, S.; Skurk, H.; Bizenberger, P.; Neske, E., "The influence of thermal diffusion on laser ablation of metal films*", Applied Physics A (Solids and Surfaces)*, **Vol. A58**, Issue 2, pp. 129-136, 1994.
6. Bloembergen. N, IEEE J. of Quantum Electron., **QE-10**, 375, 1974.
7. Schott Glass Technologies Inc., *Optical Glass Catalog*, 400 York Avenue, Duryea, Pennsylvania 18642.
8. Shah, L., "*Femtosecond laser micro-machining of glasses and polymers in air"*, Ph.D. Thesis, , University of Central Florida, Fall 2001.
9. Braun, A. ; Korn, G.; Liu, X.; Du, D.; Squier, J.; Mourou, G., "Self-channeling of high-peak-power femtosecond laser pulses in air", *Optics Letters*, **Vol. 20**, Issue 1, pp. 73-75, 1995.
10. Schaffer, C.B. ; Brodeur, A.; Garcia, J.F.; Mazur, E., "Micromachining bulk glass by use of femtosecond laser pulses with nanojoule energy", *Optics Letters*, **Vol. 26**, Issue 2 , pp. 93-95, 2001.
11. T. Cardinal, K. A. Richardson, H. Shim, A. Schulte, R. Beatty, K. Le Foulgoc, C. Meneghini, J. F. Viens, A. Villeneuve, "Non-linear optical properties of chalcogenide glasses in the system As-S-Se", *Journal of Non-Crystalline Solids*, **Vol. 256-257**, pp. 353-60, 1998.
12. Streltsov, A.M. ; Borrelli, N.F., "Fabrication and analysis of a directional coupler written in glass by nanojoule femtosecond laser pulses", *Optics Letters*, **Vol. 26**, Issue 1, pp. 42-43, 2001.

* mrichard@mail.ucf.edu; phone 407 823 6819; fax 407 823 3570; School of Optics/CREOL, University of Central Florida, 4000 Central Florida Blvd., PO BOX 162700, Orlando FL 32816.

Ablation and optical property modification of transparent materials with femtosecond lasers [5273-148]
M. C. Richardson, CREOL/Univ. of Central Florida (USA)

Q –Your beam wandering, why do you think it's preferential in one direction? From your data it looked like it was all going in the same direction. If it was a random process you would think it would wander in all directions?

A – It's a very slow process. As a function of pulses throughout the train, most probably it is random from one channel to another. Most probably it starts to guide itself.

Q – In the PMMA, did the femtosecond machining result in a positive refractive index change? Were those indeed waveguides or was the refractive index change negative?

A – We haven't yet made detailed measurements of a refractive index change in the PMMA. It's more difficult because it's in the bulk.